

[HOME](#) / [International Advisory Board](#)

International Advisory Board

[Prof. HAMEL, Rodolphe](#)

Institut de Recherche pour le Développement, Maladies Infectieuses et Vecteurs: Écologie, Génétique, Évolution et Contrôle, Montpellier, France

[Prof. MOMENI, Davood](#)

Department of Physics, College of Science, Sultan Qaboos University, Muscat, Oman

[Prof. MONTEIL, Arnaud](#)

Institut de Génomique Fonctionnelle, Centre National de la Recherche Scientifique (CNRS), Montpellier, France

[Prof. ODINTSOV, Sergey](#)

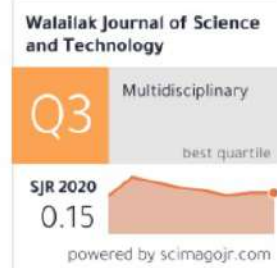
Institute of Space Sciences (IEEC-CSIC) C. Can Magrans s/n, Barcelona, Spain

[Prof. SANNINO, Francesco](#)

CP3-Origins & the Danish Institute for Advanced Study, University of Southern Denmark, Odense, Denmark

[MAKE A SUBMISSION](#)

SCIMAGO JOURNAL RANK



CITESCORE

0.7 2020 CiteScore

Effect of Feeding Different Levels of Corn Silage on Milk Yield and Quality in Dairy Assaf Ewes

Ahmed Zaazaa, Mohammed Sabbah, Tawfiq Qubbaj, Jamal Abo Omar

3044



PDF

A Gaussian Process Regression Model for Forecasting Stock Exchange of Thailand

Kamonrat Suphawan, Ruethaichanok Kardkasem , Kuntalee Chaisee

3045



PDF

Experimental Investigation of Tribological Characteristics of Blends of SGME Modified with Copper Oxide Nanoadditivation

Eknath Aitavade, Sannappa Kamate

3047



PDF

Natural Frequencies of Beams with Axial Material Gradation Resting on Two Parameter Elastic Foundation

Saurabh Kumar

3048



PDF

Design and Performance Analysis of Double Axial Flux Permanent Magnet Generator

Eko Yohanes Setyawan, Choirul Soleh, Awan Uji Krismanto, I Wayan Sujana, Soeparno Djiwo, Tutut Nani Prihatni

3049



PDF

Water Demand and Supply Analysis using WEAP Model for Veda River Basin Madhya Pradesh (Nimar Region), India

Abhay Carpenter, Mahendra Kumar Choudhary

3050



PDF

INFORMATION

[For Readers](#)

[For Authors](#)

[For Librarians](#)

VISITORS

Visitors

 IN 12,973	 MY 1,019
 ID 5,842	 BD 803
 TH 5,436	 IQ 772
 NG 1,264	 PK 729
 US 1,026	 MA 480

Pageviews: 141,796



Counter Installed 30 Sep 2021

SCHOLARSHIPS



[WU Graduate Programs](#)

[WU Scholarships](#)

Design and Performance Analysis of Double Axial Flux Permanent Magnet Generator

Eko Yohanes Setyawan¹, Choirul Soleh², Awan Uji Krismanto³,
I Wayan Sujana¹, Soeparno Djiwo¹ and Tutut Nani Prihatmi^{1,*}

¹Department of Mechanical Engineering, National Institute of Technology Malang, Indonesia

²Diploma of Electrical Engineering, National Institute of Technology Malang, Indonesia

³Department of Electrical Engineering, National Institute of Technology Malang, Indonesia

(*Corresponding author's e-mail: tutut.nani@lecturer.itn.ac.id)

Received: 9 April 2021, Revised: 16 June 2021, Accepted: 29 June 2021

Abstract

In this paper, a new permanent magnet generator structure was proposed in order to facilitate the implementation of the permanent magnet generator on small-scale renewable energy-based power generators. Detail characteristics of a double axial flux permanent magnet generator were analyzed. The proposed generator structure consisted of 2-sided rotors equipped with slots for placing permanent magnets. The stator side comprised 3 groups of coreless winding for realizing 3-phase output. Performances of the axial flux double permanent magnet generator were observed involving the output voltage, currents, and power. Two experimental scenarios have been tested to monitor the performance of the generator. In the first scenario, the loading condition which was represented by the star connection of 3 bulbs of 25 W has been considered. The rotational speed of the tested generator in this scenario was 501.9 rotation per minute (rpm). Under those loading circumstances, 3-phase sinusoidal output voltages with frequencies under 50 Hz have been monitored. Above 50 Hz operational frequency, the output voltage waveform slightly changed from sinusoidal to trapezoidal shapes. In the second scenario, the proposed generator was connected to the rectifier to form a DC system. The 45 W load has been considered in this DC scenario. Under the DC system test, 152.2 V output DC voltage, 0.1614 A current, and 24.976 W power have been monitored when the rotational speed of axial flux double permanent magnet generator was 847.9 rpm.

Keywords: Double axial, Permanent magnet generator, Renewable energy

Introduction

The axial flux permanent magnet generator was invented around 150 years ago [1]. With the increase trend of renewable energy, the permanent magnet generators design has been improving continuously to facilitate efficient energy conversion process in renewable energy-based power plant. The most popular application of permanent magnet generator involving axial flux permanent magnet generator is in small scale gearless wind generator design. It allows more compact design and efficient operation of small-scale wind conversion system. Moreover, the axial flux permanent magnet generator enables more apparent in a design with a large number of poles. Hence, low speed operation capability can be considered.

The invented generator structure has some advantages such as higher power density, better cogging torque and simple construction, resulting in more efficient and cheaper manufacturing costs [2]. Moreover, the axial flux type of generator ensures low distortion and purely sinusoidal voltage output waveform [3-5]. From a flux point of view, the geometry structure of the axial flux generator is an important feature to increase power density [6]. Effects of core shape, lamination, air-gap and core losses on the efficiency of Axial Flux Permanent Magnet Generator (AFPMG) with Finite Element Analysis (FEA) have been investigated. It was found that the dimension of the magnetic core should be minimized in order to improve efficiency and generator performances [7]. The increase in the power output of the generator can be achieved by increasing the number of coils. Therefore, in order to increase the output power without significantly change the generator construction, it is preferable to use a double-side rotor than single-side rotor configurations [9].

Enhancement of generator performance can also be achieved by considering the various configurations of the core. The core of the generator can be either slotted or slot-less which aims to reduce cogging torque and mitigate inductance losses respectively [10]. Moreover, the interaction force between the core and permanent magnet should be carefully considered to optimally reduce the cogging torque [11]. Magnetic force in axial flux generator potentially introduces larger mechanical pressure and vibration to the machine due to larger air gap in axial flux generator than in radial flux generator [9]. The air gap usually can be designed between 1 to 4 mm with considering the mechanical process of the generator. It is important to be noted that the dimension of the air gap influences the output of the generator [12]. Therefore, optimization of air gap dimension should be conducted in the design process of axial flux generators [13]. In a coreless type of rotor, the winding should be put into the non-magnetic material with isoelastic characteristics such as epoxy and polyamide. The coreless rotor type results in less weight of the generator and the absence of core loss and cogging torque. On the other hand, the drawback of the coreless type of generator is the increase of loss due to the eddy current effect in the field winding under the high-speed operation of the generator [13]. Lower magnetic fluxes which influence the efficiency of the generator also become a concern in coreless rotor type [14]. The other factor that influences the generator characteristic is the air gap. As previously mentioned, smaller air gaps would increase the output of the generator. Conversely, a higher air gap introduces more losses in generators [15].

In comparison with radial flux, axial flux permanent magnet generator has low cogging torque and higher power density and efficiency [16]. Higher power density in axial flux permanent magnet generator results in an increase in the operating temperature of the generator. Therefore, in axial flux generators, air gap design is important to reduce the operating temperature [17-21]. In order to achieve good generator performance in axial flux permanent magnet generator, stator and rotor design should be combined properly to reduce the power loss and increase efficiency [7,8]. Two side rotor design can be considered to increase the power output of the generator. Since the proposed design doubled the generator output power [22].

With all the benefits and limitations of an axial flux permanent magnet generator, it is important to find a suitable design in order to increase efficiency while maintaining the power quality of the machine. As mentioned before, a number of rotors potentially increase the power output without increase the dimension of the machines, hence it would not increase the cost significantly. In this paper, the characteristics and performance of the double-sided axial flux permanent magnet generator were comprehensively analyzed. The proposed generator considers 2 side rotor design with a permanent magnet. Moreover, in order to maintain power quality, the output of the generator is connected to the rectifier to converse AC terms output into DC terms output. The main contributions of the paper are proposing a simple design of double flux permanent magnet generator and providing a comprehensive analysis of the proposed generator. Moreover, it provides practical experimental setups to investigate and enhance the performance of the generator. The remainder of the paper is presented as follows: Experimental setup and methods are presented in Section II; the obtained results and discussions are given in Section III. Eventually, the conclusions were presented in Section IV.

Materials and methods

The design procedure of the double-sided axial flux permanent magnet generator is shown in **Figure 1**. The proposed double axial flux permanent magnet generator would be implemented to a renewable energy-based generation system that naturally has fluctuating features, intermittency and uncertain resource availability. With all those uncertainties, it is necessary to ensure a stable operation and power quality of renewable energy-based power generation. In order to mitigate the distortion of output voltage and reduce the harmonic content as a consequence of implementing unpredictable energy resources, the DC system was proposed. To facilitate power conversion from AC to DC form, the output terminal of the generator was connected with a rectifier to provide the DC voltage and current output. The proposed DC system was shown in **Figure 1(a)**.

Performance of double axial permanent magnet generator was observed in no-load and loading scenarios. The loading scenario moreover, considered AC and DC loads in order to compare the performance of the proposed generator. The AC and DC loads were presented in terms of the DC and AC bulbs respectively. The output voltage, current and power were carefully monitored through an oscilloscope system. Furthermore, to obtain the comprehensive characterization of the machine at various rotational speeds, the shaft of the proposed generator was coupled with an adjustable speed electric motor. The experimental setup was depicted in **Figure 1(b)**. In this paper, the double rotor design was selected to

improve the performance and increase the power output of the permanent magnet generator. The 3D design of the double axial permanent magnet generator was shown in **Figure 1(c)**.

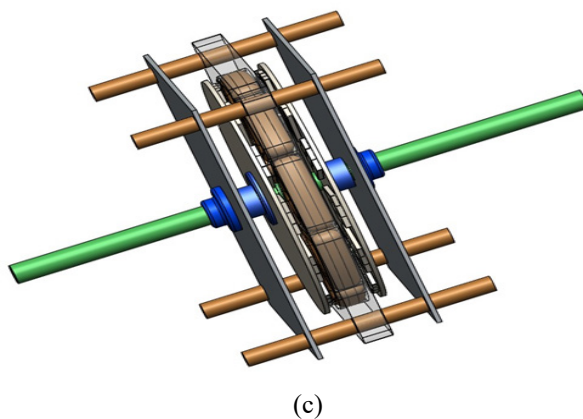
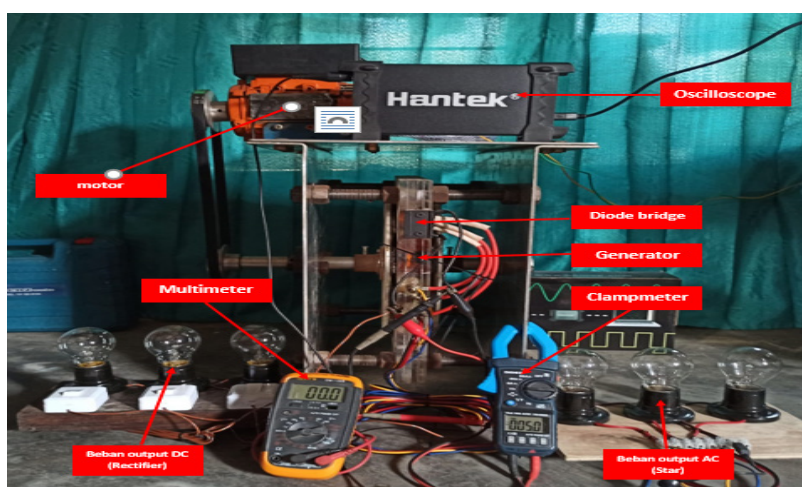
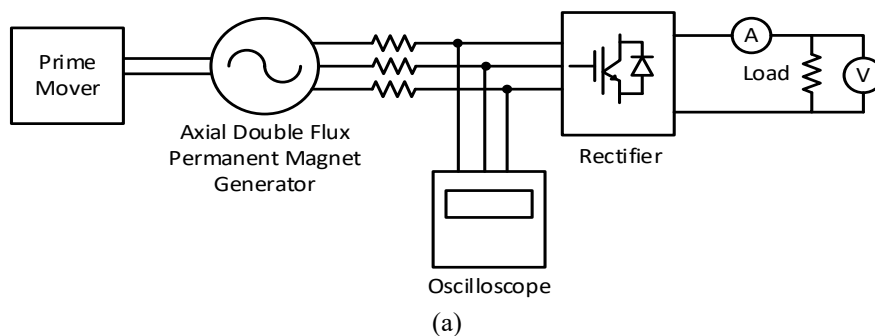


Figure 1 Design and experimental setup of double side axial flux permanent magnet generator. (a) diagram of proposed double side axial flux permanent magnet generator (b) experiment setup of double side axial flux permanent magnet generator (c) the design of double side axial flux permanent magnet generator.

A detailed design of the double-side rotor in the proposed axial flux generator was depicted in **Figure 2**. In this research, the dimension of the generator has a length of 45 cm length, a width of 33 cm, and a height of 46 cm. The purpose of the small size design of the generator was to facilitate flexibility, simple installation and portable features. The proposed rotor design incorporates a double rotor type in

the left and right of the stator. The rotors and stators were connected with a shaft to rotate at a similar speed and direction. On each side of the rotor, 12 permanent magnets of neodymium type with $50 \times 15 \times 6$ mm³ dimension were installed. Therefore, inside the generator, there were 24 permanent magnets on the rotor side.

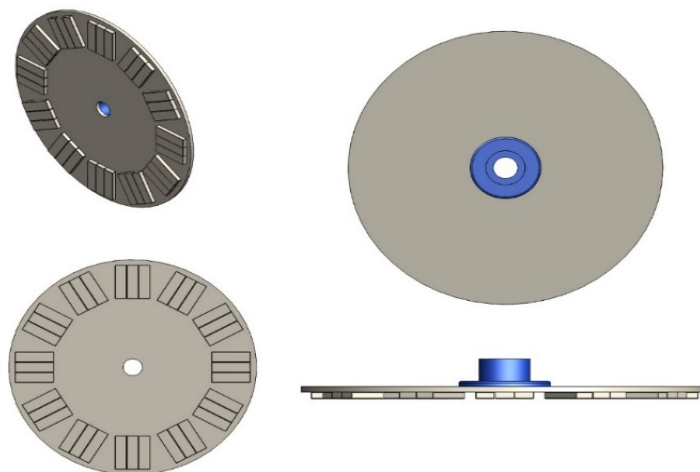


Figure 2 Design of double-side rotor in proposed axial flux generator.

The stator side of the proposed permanent magnet generator is the copper winding with the number of windings is 9. Since the output of the generator is 3-phase, the windings are divided into 3 groups. Each group consisted of 3 winding. The conductor used in this design was a copper conductor with a 1 mm diameter. The number of turns in each winding was 300 turns. Moreover, the air gap between the rotor and stator was determined as 4 mm. The stator design of the double-sided axial flux permanent magnet generator was shown in **Figure 3**.

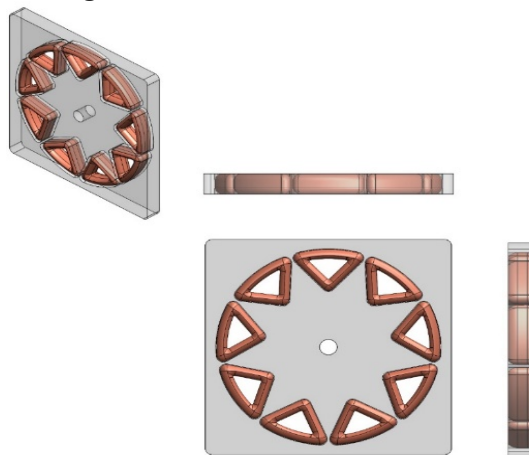


Figure 3 Stator design of double-sided axial flux permanent magnet generator.

The proposed design of the double-sided axial flux permanent magnet generator has an efficient natural cooling mechanism in the surface of the stator and rotor. The configuration of the permanent magnet was symmetric and parallel with the position of the stator winding with pole orientation of N-S-N-S. The pole orientation of rotor was complementary to each other.

In 3 phase constructions, the windings which was connected in series, was further divided into 3 different groups. Each group represented 1-phase output of the generator. It was compulsory to produce 3 identical output waveforms with similar phase angle to ensure a good quality of generator power output. Therefore, each group of winding should have identical shape, type of winding and number of turns. Total inductance in each phase can be stated as follows:

$$L_{\text{phase}} = L_1 + L_2 + L_3 + \dots + L_n \quad (1)$$

L_{phase} represents a total inductance in each phase and L_1, L_2, L_3 and L_n are inductance values in each winding. n is the number of windings connected in series in single phase.

Involving the terminal output voltage in each phase, load voltage and voltage drop along the winding, the voltage relationship in each phase can be represented using the following equation:

$$V_{\text{phase}} - V_{\text{Rphase}} - V_{\text{Lphase}} = 0 \quad (2)$$

V_{phase} is phase voltage. While V_{Rphase} and V_{Lphase} represent load voltage and voltage drop of the winding respectively.

The Eq. (2) can be rewritten as a function of currents and impedance as given in the following equation:

$$\frac{di_A}{dt} = \frac{i_A}{L_{pA}} (R_A + R_{LA}) \quad (3)$$

i_A is phase current. L_{pA} is the total impedance of each phase. R_A and R_{LA} represent the load and winding resistance respectively.

Induction voltage in each phase is stated using the following equation:

$$V_{LpA}(t) = -3N \frac{d\theta(t)}{dt} \quad (4)$$

The coefficient of 3 represents number of groups winding that are connected in similar phase and N represents number of turns in each winding.

The power output of the generator was stated as follows:

$$P_{\text{out}} = 3 V(t) \cdot i(t) \quad (5)$$

$V(t)$ and $i(t)$ represent the instantaneous voltage and current respectively. The power factor was assumed as unity power factor.

In balance multi-phase system, the total output power can be determined by multiplying the single-phase output with the coefficient number which represent the number of phases. Hence, the total output power in multi-phase system is stated as follows:

$$P_{\text{out}} = m \cdot V(t) \cdot i(t) \quad (6)$$

m represents the number of output phase.

As previously mentioned, power losses in generator is comprising of copper losses in the winding, core loss in permanent magnet and mechanical loss [10,17]. As the main windings are located in stator, the power losses depend on the design of the stator. The total copper loss can be stated using the following equation:

$$P_{\text{cu}} = m \cdot i(t)^2 \cdot R_p \quad (7)$$

In general, core loss is consisting of hysteresis, eddy current and anomalous losses [23]. The core lost can be presented as follows:

$$P_{\text{Fe}} = P_h + P_e + P_a \quad (8)$$

$$P_h = k_h \frac{f}{50} B_{pk}^{1.8} W_{fe} \quad (9)$$

$$P_e = k_e \left(\frac{f}{50} B_{pk} \right)^2 W_{fe} \quad (10)$$

$$P_a = k_a \left(\frac{f}{50} B_{pk} \right)^{1.5} W_{fe} \quad (11)$$

P_e , P_{Fe} , P_h and P_a represented the eddy current, core, hysteresis and anomalous losses respectively. W_{Fe} represented core mass, B_{pk} represented the peak of flux density in Tesla. While k_a , k_e and k_h represented the coefficient constant of anomalous loss, eddy loss and hysteresis loss respectively. According to the previous equations, the total efficiency of the generator (ΔP) can be stated as follow:

$$\eta = \frac{P_{out}}{P_{out} + \Delta P} \cdot 100 \quad (12)$$

Results and discussion

The first experimental setup considered a loading condition with resistive loads. Specifically, 3 bulbs of 25 W in star configuration have been considered in this scenario. The waveforms of the terminal voltage at the output AC side of the generator were monitored. It is important to monitor the voltage waveform and quality of AC terminal of the generator to decide whether further process such as filtering or rectification are required. Moreover, the rotational speed is increased gradually to determine the nominal operational speed of the proposed generator in 50 Hz nominal frequency.

Table 1 represented the monitoring results of the AC side generator terminal voltages. It was observed that the phase voltages of the generator had relatively similar magnitude values. The small difference of those magnitude values might be caused by some factors such as the shape of the coil which was not perfectly identic and non-uniform air gap distance which results in fluctuating effects of inductance values between permanent magnet and coil. Moreover, it was monitored that the terminal voltage of the generator was increasing proportionally with the increase of the rotational speed. As the speed was increasing, the frequency output of the generator also increased. It was monitored that the proposed generator can be operated in nominal frequency of 50 Hz in 501.9 rpm rotational speed.

Table 1 Measurement of the output voltage of each generator phase.

RPM	R-N (V)	S-N (V)	T-N (V)	Frequency (Hz)
204	17,4	16	17	20,5
305,8	25,9	23,7	25,3	30,5
417,2	32,7	29,9	32,2	41,4
501,9	39,7	36,1	38,7	50,1
612,7	48,7	44,5	47,6	60,9
718,7	56,1	51,1	54,7	70,5
807,7	63,3	57,6	61,7	80,5
894,2	71,7	65,5	70,1	90
1010,4	81,2	74,1	79,4	100,7
1141,7	89,1	81,3	87,1	110,7

Figure 4 presented the 3-phase AC side voltage waveform of the axial double flux permanent magnet generator. It was monitored that in 240 rpm rotational speed, the waveform of the AC side output voltage was purely sinusoidal with the operating frequency is 20.5 Hz. The voltage magnitude of phase R was 17.4 Volt, phase S 16 Volt and phase T is 17 Volt. **Figure 5** presented the 3-phase AC side voltage waveform of the axial double flux permanent magnet generator when it was operated at 417.2 rpm rotational speed. Similarly, it was monitored that the waveform of the AC side output voltage was purely sinusoidal with an operating frequency of 41.4 Hz. Moreover, the voltage magnitude of phase R was 32.7 Volt, phase S 29.9 Volt, and phase T was 32.2 Volt.

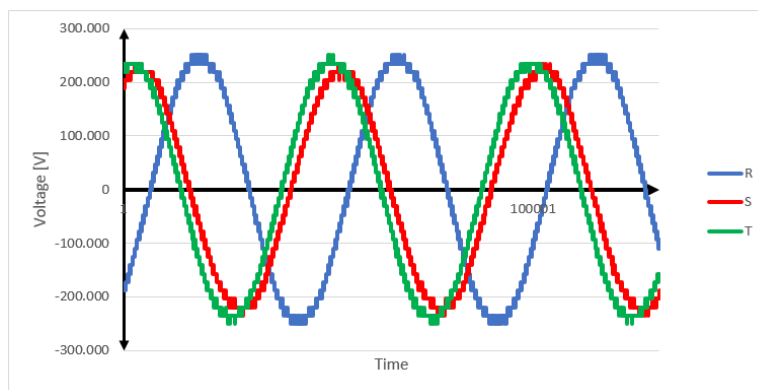


Figure 4 Three phase voltage output at frequency of 20.5 Hz.

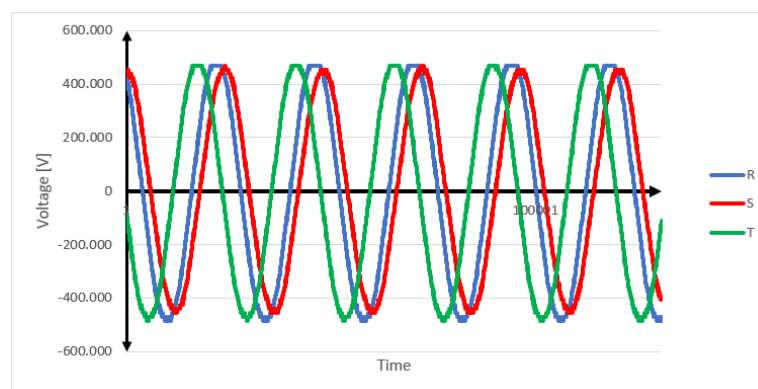


Figure 5 Three phase voltage output at frequency of 41.4 Hz.

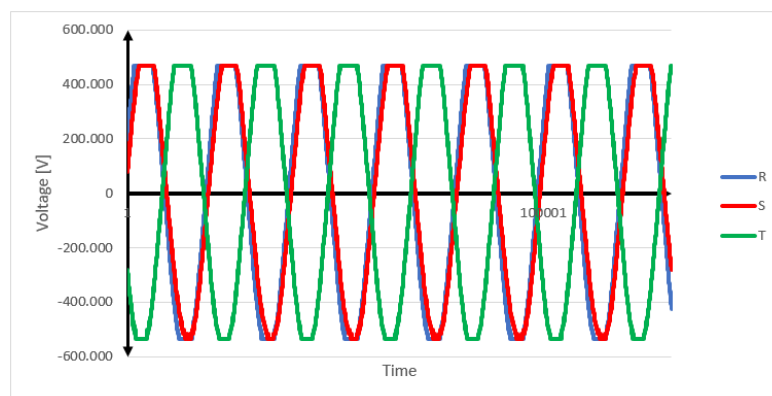


Figure 6 Three phase voltage output at frequency of 50.1 Hz.

Figure 6 presented the 3-phase AC side voltage waveform of the axial double flux permanent magnet generator under 501.9 rpm rotational speed. In this rotational speed, the operating frequency of the generator was 50.1 Hz, similar to the fundamental frequency of the utilities. Therefore, it can be observed that the proposed axial double flux permanent magnet generator can be synchronized with the grid within this rotational speed. The waveform of the AC side output voltage was purely sinusoidal. The voltage magnitude of phase R was 39.7 Volt, phase S 26.1 Volt and phase T was 38.7 Volt. As the rotational speed was continuously increased to 612.7 rpm, the operational frequency changed to 60.1 Hz. The waveform of the generator terminal voltages was changing into trapezoidal form as presented in Figure 7, with the magnitude of phase voltage was 48.7 Volt for phase R, 44.5 Volt for phase S and 47.6 Volt for phase T.

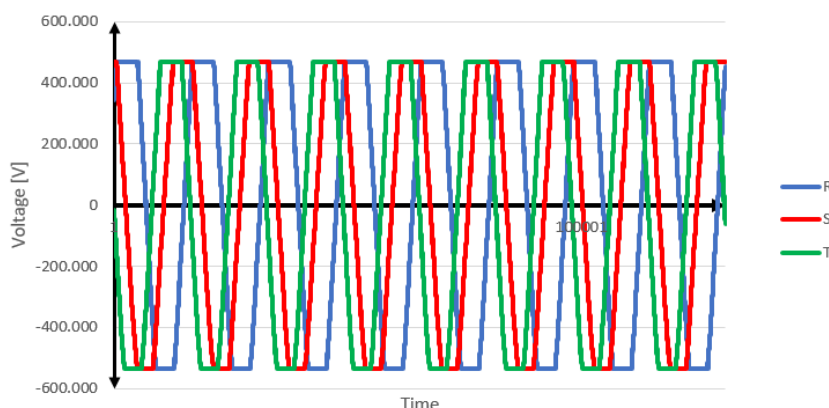


Figure 7 Three phase voltage output at frequency of 60.9 Hz.

As presented in Figures 4 - 7, it was clearly observed that there were some concerns regarding the terminal output voltage at the AC side of the generator. The limitation of the manufacturing process resulted in the unbalanced position of the coil and non-uniform air gap. Consequently, the phase angle among phase voltage was not equal. In ideal conditions, the phase voltage should be separated by 120 to each other. However, the obtained results indicated an unbalanced condition of phase shift among those 3-phase voltages. The unbalanced in-phase voltages disturbed the current waveform significantly and deteriorated the power quality. Moreover, as rotational speed is increased, more deviation and distortion of voltage waveforms were monitored, indicated by a change of voltage waveforms from purely sinusoidal to trapezoidal shapes. The distorted voltage and current waveform increased the harmonic content in the system. High harmonic content would result in an increase in losses and heating problems. With those concerns, it is not allowed to directly connect the AC side terminal voltage of the proposed axial flux permanent magnet generator to the load. To solve the problem, the power quality and the distortion of AC side terminal voltages need to be improved. Among several options such as connecting an additional low pass filter at the AC side of the generator and drastically change the construction of the generator, it is preferable to convert the distorted AC form into free-distortion DC form voltage and current.

In second scenario, the AC side terminal generator was connected to a full bridge rectifier to overcome the power quality and mitigate the distortion problems of AC terminal voltage of the generator. To analyze the performance of the proposed generator and coupling the full-bridge rectifier, 2 experimental setups were used. The first experimental setup used a constant loading condition with a 45 W bulb and the second experimental setup considered fluctuating loading conditions. Figure 8 shows the correlation between rotational speed and DC voltage. Under constant loading condition, it was observed that the DC voltage was increasing proportionally with the increase of rotational speed. Higher rotational speed resulted in higher DC voltage. Consequently, as the DC voltage was increasing with the increase of rotational speed, the power output of the current also proportionally increasing as shown in Figure 9.

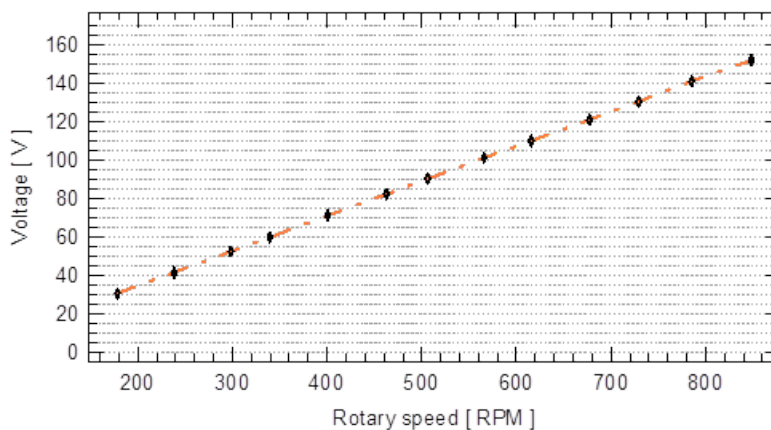


Figure 8 Correlation between rotational speed and DC voltage.

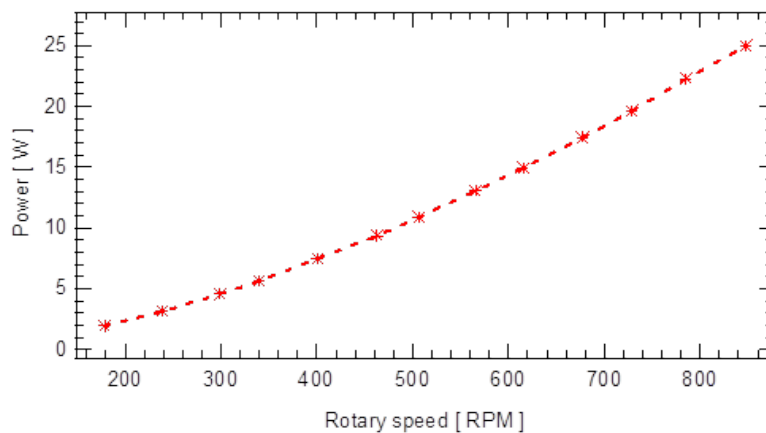


Figure 9 Correlation between output power and rotational speed.

The second experimental setup for DC configuration of permanent magnet generator with rectifier analyzed the generator performance under load variations scenario. The correlation between output power as the function of the load is shown in **Figure 10**. The connected load was increasing gradually from 15 to 45 W with a constant rotational speed of 840 rpm. The output power was continuously increasing with the increase of connected load. At a loading condition of 15 W, the output power was 8.514 W. At a 25 W loading condition, the measured output power was 13.520. Under 30 and 40 W loading circumstances, the output powers of the generator were 16.314 and 22.948 W respectively. Finally, at 45 W of load, the measured output power was 45 W.

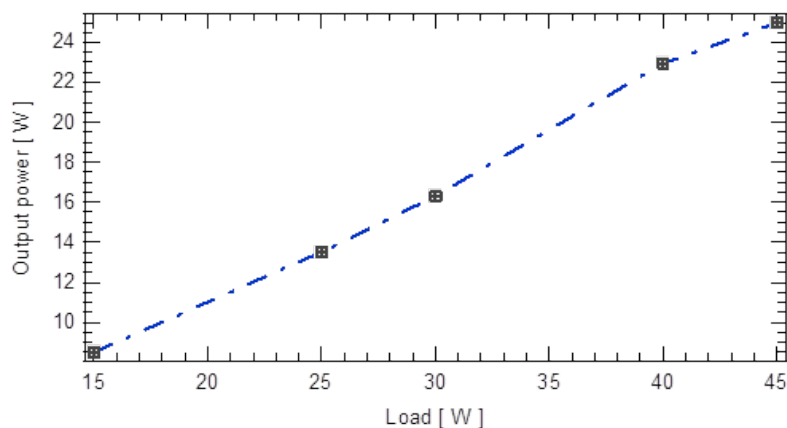


Figure 10 Correlation between output power and rotational speed.

Conclusions

Design and experimental assessment of double axial flux permanent magnet generator were presented in this paper. The experimental results suggested that the AC side terminal voltage of the proposed generator has an unbalance phase shift and high distortion when it was operated at a higher rotational speed. To overcome the problem, the proposed generator was connected with a full bridge rectifier to generate DC form voltage and output power. From the experimental results, it was clearly monitored that the voltage of the generator can be increased by increasing the rotational speed. Therefore, the voltage can be controlled and regulated by adjusting the rotational speed of the generator.

Acknowledgements

The authors are grateful to the Institute for Research and Community Engagement (LPPM), National Institute of Technology Malang, Indonesia for providing support.

References

- [1] M Sadeghierad, H Lesani, H Monsef and A Darabi. Detail modeling of high-speed axial flux PMG. *Aust. J. Basic Appl. Sci.* 2009; **3**, 1467-75.
- [2] SP Barave and BH Chowdhury. Optimal design of induction generators for space applications. *IEEE Trans. Aero. Electron. Syst.* 2009; **45**, 1126-37.
- [3] E Kurt, S Aslan and M Demirtas. Cogging torque exploration of radially and angularly directed fluxes in a new PM generator with the multiple stators. *In: Proceedings of the 7th International Conference and Exhibition on Ecological Vehicles and Renewable Energies - EVER, Monte Carlo, Monaco.* 2012.
- [4] E Kurt and H Gör. Comparison of cogging torques in two different axial flux permanent magnet generators. *In: Proceedings of the 2nd European Workshop on Renewable Energy Systems, Antalya, Turkey.* 2013.
- [5] E Kurt and H Gör. Electromagnetic design of a new axial flux generator. *In: Proceedings of the 6th International Conference on Electronics, Computers and Artificial Intelligence (ECAI), Bucharest, Romania.* 2014, p. 39-42.
- [6] H Vansompel, P Sergeant, L Dupre and AV Bossche. Axial-flux PM machines with variable air gap. *IEEE Trans. Ind. Electron.* 2014; **61**, 730-7.
- [7] GF Price, TD Batzel, M Comanescu and BA Muller. Design and testing of a permanent magnet axial flux wind power generator. *In: Proceedings of the 2008 IAJC-IJME International Conference, Tennessee, United States.* 2008, p. 190-202.
- [8] D Patterson and R Spee. The design and development of an axial flux permanent magnet brushless DC motor for wheel drive in a solar powered vehicle. *IEEE Ind. Appl.* 1995; **31**, 1054-61.
- [9] SY Sung, JH Jeong, YS Park, JY Choi and SM Jang. Improved analytical modeling of axial flux machine with a double-sided permanent magnet rotor and slotless stator based on an analytical method. *IEEE Trans. Magn.* 2012; **48**, 2945-8.
- [10] BJ Chalmers and E Spooner. An axial-flux permanent-magnet generator for a gearless wind energy system. *IEEE Trans. Energ. Convers.* 1999; **14**, 251-7.
- [11] M Aydin and MK Guven. Design of several permanent magnet synchronous generators for high power traction applications. *In: Proceedings of the 2013 International Electric Machines & Drives Conference, Chicago, United States.* 2013, p. 81-7.
- [12] M Sadeghierad, H Lesani, H Monsef and A Darabi. Design considerations of high-speed axial flux permanent magnet generator with coreless stator. *In: Proceedings of the 2007 International Power Engineering Conference, Singapore.* 2007, p. 1097-102.
- [13] TD Nguyen, KJ Tseng, S Zhang and HT Nguyen. A novel axial flux permanent-magnet machine for flywheel energy storage system: Design and analysis. *IEEE Trans. Ind. Electron.* 2011; **58**, 3784-94.
- [14] RJ Wang and MJ Kamper. Calculation of eddy current loss in axial field permanent magnet machine with coreless stator. *IEEE Trans. Energ. Convers.* 2004; **19**, 532-8.
- [15] Y Chen, P Pillay and A Khan. PM wind generator comparison of different topologies. *In: Proceedings of the 39th Conference Record of the IEEE Industry Applications Society Annual Meeting, Washington, United States.* 2004, p. 1405-12.
- [16] N Al-Aawar, TM Hijazi and AA Arkadan. Design optimization of axial-flux permanent magnet generator. *In: Proceedings of the Digests of the 2010 14th Biennial IEEE Conference on Electromagnetic Field Computation, Chicago, United States.* 2010.
- [17] JR Bumby and R Martin. Axial-flux permanent-magnet air-cored generator for small-scale wind turbines. *IEE Proc. Electr. Power Appl.* 2006; **152**, 63-73.
- [18] E Kurt, H Gör and M Demirtaş. Theoretical and experimental analyses of a single phase permanent magnet generator (PMG) with multiple cores having axial and radial directed fluxes. *Energ. Convers. Manag.* 2014; **77**, 163-72.
- [19] CC Chan. Axial-field electrical machines-design and applications. *IEEE Trans. Energ. Convers.* 1987; **2**, 294-300.
- [20] MA Ezzat and AA El-Bary. Two-temperature theory of magneto-thermo-viscoelasticity with fractional derivative and integral orders heat transfer. *J. Electromagn. Waves Appl.* 2014; **28**, 1985-2004.
- [21] MA Ezzat, AS El-Karamany, AA El-Bary and MA Fayik. Fractional ultrafast laser-induced magneto thermoelastic behavior in perfect conducting metal films. *J. Electromagn. Waves Appl.* 2014; **28**, 64-82.

- [22] TF Chan, W Wang and LL Lai. Magnetic field in a transverse and axial-flux permanent magnet synchronous generator from 3-D FEA. *IEEE Trans. Magn.* 2012; **48**, 1055-8.
- [23] TF Chan, LL Lai and S Xie. Field computation for an axial flux permanent-magnet synchronous generator. *IEEE Trans. Energ. Convers.* 2009; **24**, 1-11.